Received: 12 December 2023 | Revised: 7 April 2024 | Accepted: 12 April 2024

DOI: 10.1002/pld3.586

RESEARCH ARTICLE

Analysis of ginseng rusty root symptoms transcriptome and its pathogenesis directed by reactive oxygen species theory

Pengcheng Yu | Xiaowen Song | Wei Zhang | Yao Yao | Junling Ren | Liyang Wang | Wenfei Liu | Zhaoping Meng | Xiangcai Meng

Country College of Pharmacy, Heilongjiang University of Chinese Medicine, Harbin, China

Correspondence
Xiangcai Meng, Country College of Pharmacy, Heilongjiang University of Chinese Medicine, Harbin, 150006, China.
Email: mengxiangcai000@163.com

Funding information
This research was supported by the National Natural Science Foundation of China (grant number: 20012210001) and the University Nursing Program for Young Scholars with Creative Talents in Heilongjiang Province (grant number: UNPYSCT-2020224).

Abstract

Ginseng rusty root symptoms (GRS) is a primary disease of ginseng, which seriously decreases the yield and quality of ginseng and causes enormous losses to ginseng production. GRS prevention and control is still challenging due to its unclear etiology. In this study, the phloem tissue of healthy *Panax ginseng* (AG), the nonred tissue of the phloem epidermis around the lesion (BG), and the red lesion site tissue of GRS (CG) were extracted for mRNA transcriptomic analysis; 35,958 differentially expressed genes (DEGs) were identified and were associated with multiple stress resistance pathways, reactive oxygen species (ROS), and iron ion binding. Further study showed that the contents of $O_2^{\bullet-}$, H_2O_2, and malondialdehyde (MDA) were significantly increased in BG and CG tissues. Under anaerobic conditions caused by excessive soil moisture, the overproduction of ROS destroys cell membranes, simultaneously converting Fe^{2+} to Fe^{3+} and depositing it in the cell wall, which results in GRS, as evidenced by the success of the GRS induction test.

KEYWORDS
ginseng rusty root symptoms; GSEA, Fe^{3+}; ROS; transcriptomics

1 | INTRODUCTION

Ginseng is a well-known botanical medicine from *Panax ginseng* C.A. Meyer, which has been used medicinally for thousands of years in China, Korea, Japan, and other Asian countries (Proctor & Bailey, 1987). Ginseng contains saponins, polysaccharides, volatile oil, and other active ingredients, with pharmacological effects of neuromodulation, cardiovascular regulation, anti-injury, anti-inflammation, antitumor, anti-obesity, and others (Fan et al., 2021; Li et al., 2021). *P. ginseng*, as a shady plant with long growth, has high requirements for the growth environment, prefers humidity and weak acidic soil with good ventilation (pH 4–6), and fails to tolerate excessive moisture. (Shin et al., 2021). Ginseng rusty root symptoms (GRS) is a common disease of ginseng (Figure 1). In diseased plants, the root epidermis is covered with rough, irregular rust-like red patches with different depths and cracks (Liu et al., 1998; Zhao et al., 1999). Several studies have shown that Fe^{3+} content is significantly increased in GRS compared with healthy ginseng, which is also the main reason for the red rust color of GRS. (Lee et al., 2011; Li et al., 1999; Wang, Sun, Xu, Ma, Li, Shao, Guan, Liu, & Liu, 2019; Zhang et al., 2016). During GRS, the contents of active ingredients such as ginsenosides significantly decreased, seriously reducing ginseng quality and yield (Guan et al., 2022). In the 1990s, the economic loss caused by GRS was as high as millions of dollars, and the incidence rate has remained high in recent years (Zhao et al., 2022). In areas with a high incidence of GRS, environmental conditions often include high soil moisture, excessive

FIGURE 1 Ginseng rusty root symptom (GRS) (left) and healthy ginseng (right).

metal ions, and high microbial abundance. Some studies have shown that GRS is an infectious disease (Wei et al., 2020), while others have demonstrated that GRS is a physiological disease caused by soil condition deterioration (Wang et al., 2016) and metal ion stress (Farh et al., 2017). The essential etiology of GRS so far is not clear, and the prevention and control of GRS is still a challenge. However, whether it is a physiological or invasive disease, they all have one thing in common: ecological coercion, which leads to metabolism changes. These diseases are associated with stress, and stress inevitably leads to a significant increase in reactive oxygen species (ROS). ROS are a class of oxygen-containing molecules, including $O_2^{\bullet-}$, H_2O_2, and ·OH, with a high active and oxidizing capacity (Gill & Tuteja, 2010), which is a fundamental reason for plant damage (Mansoor et al., 2022; Yana et al., 2017). It has been shown that ROS can oxidize and decompose the long-chain fatty acids in the phospholipid bilayer of the cell membrane and destroy the carbon chain (Garg & Manchanda, 2009). The red-skin components $Al_3Cl(CH_3COO)_5 \cdot 1.5\ CH_3COOH$, $C_{13}H_{21}Al_3O_{13}$, $C_{14}H_{10}Fe_2NS_2$, and other complexes have a small C: H ratio or two carbon molecules (Garg & Manchanda, 2009; Zhao, 1998), suggesting that they are likely to be the product of cell membrane damage. In addition, the H_2O_2 content in the red-skin area of ginseng is increased, and the activities of antioxidant enzymes such as superoxide dismutase, catalase, and phenolic compounds are increased accordingly (Zhou et al., 2017). This also suggests an association between GRS and ROS, originating from stress.

Transcriptomics can provide insights into gene transcription and transcriptome regulation in cells at an integrative level (Lowe et al., 2017): The transcriptome can reflect the dynamic genes expression of cells at a specific stage and under one particular environment, unearth functional genes, reveal the regulation of secondary metabolic networks and molecular markers, and more comprehensively reveal the nature of the growth and development of medicinal plants, stress resistance, and the influence of various metabolic environments on metabolism (McGettigan, 2013; Wan et al., 2011). Bian et al. (2021) conducted a transcriptomic study on ginseng and performed Gene Ontology (GO) and Kyoto Encyclopedia of Genes and Genomes (KEGG) analyses. They found that several stress-related pathways, such as phenylpropanoid biosynthesis, peroxisome, plant-pathogen interaction, and plant hormone signal transduction, were upregulated in GRS ginseng. However, the results of Bian et al. only describe the phenomena after the occurrence of GRS, fail to clarify the causality and parallels between various indicators, or find the underlying cause of these phenomena, due to the limitation of GO and KEGG analyses, which can only locate gene function. Therefore, in our study, we used a transcriptome study with a focus on ROS and added a macro gene set enrichment analysis (GSEA) analysis to examine the expression level of overall gene sets instead of individual genes (Hung et al., 2012). Targeted research on the relationship between stress-induced ROS of rusty ginseng and the expression of the overall gene set can more accurately reveal the biological nature of rusty ginseng. In addition, the nonred tissue of the phloem epidermis around the lesion was added as a sample for this study, which more clearly showed the genetic changes in the transition state from healthy ginseng to rusty ginseng. Meanwhile, $Na_2S_2O_4$ (Carrier of $O_2^{\bullet-}$) induced the occurrence of GRS, further demonstrating that ROS is the essential cause of GRSs.

2 | MATERIALS AND METHODS

2.1 | Collection of plant materials

All the plant experiments complied with relevant institutional, national, and international guidelines and legislation. Cultivated *P. ginseng* (RS2022081) collection was done with permission. All ginseng samples (5 years old), identified by Prof. Xiang-Cai Meng of the Heilongjiang University of Chinese Medicine, were collected in Baishan City, Jilin Province, China (42.17 N and 127.48E) in August 2022 (the rainy season with high incidence of GRS). Healthy phloem tissue (AG), phloem tissue around red plaques of GRS (BG), and red plaques tissue of GRS (CG) were collected immediately, frozen with liquid nitrogen, and stored at −80°C. Three independent biological replicates were prepared for each group, and each replicate included individuals from five or more roots, which were collected in different periods.

2.2 | RNA isolation

Nine complementary DNA (cDNA) libraries were constructed: three for AG tissues, three for BG tissues, and three for CG tissues. Total RNA was extracted and isolated from each sample using an RNA extraction kit (Tian gen, Beijing, China). RNA concentration and purity were

measured using a NanoDrop 2000 spectrophotometer (Thermo Fisher Scientific, Waltham, MA, USA). RNA integrity was assessed using an Agilent 2100 bioanalyzer (Agilent Technologies, Santa Clara, CA, USA).

2.3 | Construction and quality control of transcriptome libraries

The 3 μg of RNA per sample was used as the input material for RNA sample preparation. mRNA was separated from total RNA and purified by mRNA Capture Beads (Vazyme, Nanjing, China). The purified mRNA was incubated in a preheated Polymerase chain reaction (PCR) instrument (Life Technologies, CA, USA) at 94°C for 7 min, interrupted, cooled immediately after the interruption, and centrifuged. The first strand of cDNA was synthesized using the supernatant containing fragment RNA as the template. The double-strand synthesis reaction reagents were added to the first strand product of the synthesized cDNA, mixed, centrifuged, and incubated in a metal bath to synthesize the second strand. Magnetic beads were used to purify the double-strand cDNA product. After adapter ligation, the fragments were screened by DNA clean beads (Vazyme, Nanjing, China), and the library was enriched by PCR using the screened cDNA fragments as templates.

Qubit 3.0 fluorescence quantifier (Thermo Fisher Scientific, Waltham, MA, USA) was used for preliminary quantification until the concentration reached more than 1 ng/μL. The Qsep400 high throughput analysis system was used to detect the inserted fragments of the library. After the pieces were inserted as expected, Q-PCR was used to accurately quantify the effective concentration of the library (effective concentration>2 nM).

2.4 | Transcriptome sequencing, data assembly, and quality control

A sequence was performed by Biomarker Technologies Co., Ltd (Beijing, China). Qualified libraries were sequenced in PE150 mode using the Illumina novaseq6000 high-throughput sequencing platform (Illumina, San Diego, CA, USA). The raw RNA-seq data are available at https://dataview.ncbi.nlm.nih.gov/object/PRJNA993718?reviewer=j4dq5solvftnkl319f5ppi950s in read-only format. The resulting Raw Data were provided in fastq format, and high-quality Clean Data was obtained after filtering low-quality Reads.

The Q30 and GC contents of clean data were calculated simultaneously. Trinity software (Grabherr et al., 2011) breaks sequencing Reads into shorter fragments (K-mer), then extends these smaller fragments into longer fragments (Contig), and utilizes the overlap between these fragments into Component sets to identify transcribed sequences in each fragment set, complete data assembly and obtain Unigene libraries. The N50 length was calculated to evaluate the quality of the data assembly, the length of the series from large to small, and the length of the cumulative line when the length exceeds 1/2 of the total length.

2.5 | Differentially expressed gene (DEG) analysis and functional annotation

DESeq2 software (Love et al., 2014) was used to screen DEGs among sample groups based on the count value of genes in each sample. Fold change (FC) ≥ 2 and false discovery rate (FDR) < .01 were considered as DEGs. FDR was obtained by correcting the difference significance *p*-value, and FC represents the expression ratio between two samples. Based on this, GO, KEGG, and GSEA were performed using BMKCloud (www.biocloud.net).

2.6 | Quantitative real-time PCR

According to the gene expression levels and differences between samples, six genes were randomly selected for quantitative real-time (qRT-PCR) verification by using qTOWER 2.2 Quantitative Real-Time PCR Thermal Cyclers (Analytik Jena GA, Jena, Germany). All of the primers used in this study are listed in Table 1. Three biological replicates were performed, and the relative RNA expression was calculated using the $2^{-\Delta\Delta Ct}$ method.

2.7 | Determination of $O_2^{\bullet-}$, H2O2 and MDA

The plant tissue was accurately weighed, and the extraction solution was added according to the weight-to-volume ratio of 1:9. After grinding under the ice bath, the homogenate was centrifuged at 2500 rpm/min for 10 min. The contents of $O_2^{\bullet-}$, H_2O_2, and MDA were determined according to the instructions ($O_2^{\bullet-}$ content detection kit: Solarbio, Beijing, China; H_2O_2 and MDA content detection kit: Jiancheng, Nanjing, China), respectively, and the determination was repeated three times.

TABLE 1 Primer sequences of the genes for qPCR verification.

Gene	Primer	Sequence
ACTIN	Forward	5'-CAACCATAAACGATGCCGA-3'
	Reverse	5'-AGCCTTGCGACCATAC-3'
104256	Forward	5'-ATCTCTCAGTCCCTGTAGAAAGA-3'
	Reverse	5'-GAATGACGACCGAAGCAGT-3'
111443	Forward	5'-CGTATCAGTGAAAGCAACAT-3'
	Reverse	5'-TTGGAGAAGAGGAATGGC-3'
076652	Forward	5'-GCTACGGTGTCATCACTAAC-3'
	Reverse	5'-TCCCATAGCCAACTTTCAGA-3'
007124	Forward	5'-CAACGCCTGCTGTGATAAG-3'
	Reverse	5'-CAGATCCACTCGGGTATGAC-3'
005058	Forward	5'-GTCGTTCTGAATCCCTACTG-3'
	Reverse	5'-TTTCCATCGGTGCCAAAT-3'
073540	Forward	5'-GGTCTTGTATATCTTCTGGTTACG-3'
	Reverse	5'-GATGAGGGTGGCAAACAG-3'

2.8 | Validation of ROS-induced GRS

The soil was collected from farm, where GRS had never occurred. Selected healthy ginseng were planted in pots, irrigated with 15 mmol/L $Na_2S_2O_4$ solution (the carrier of $O_2^{\bullet-}$) to saturation, and covered with plastic wrap to simulate a hypoxic environment. After 20 days, the ginseng was dug out and photographed.

2.9 | Statistical analysis

Statistical analysis was performed with SPSS 20.0 software. The data were expressed as the mean ± standard deviation (SD). $p < .05$ was considered to be statistically significant.

3 | RESULTS

3.1 | Sequencing and assembly of transcriptomics

A total of 55.86 Gb of high-quality Clean Data was obtained by transcriptome sequencing of 9 samples, and the Clean Data of all models reached more than 5.87 Gb. The contents of the Q30 base were more than 92.93%, and the contents of the GC base were between 42.71% and 43.73% (Table 2). The assembly obtained a total of 915,750 transcripts (Table 3). The total sequence length was 1264342025bp, the average size was 1380.66 bp, and the N50 was 2033 bp. A total of 99,944 Unigenes were obtained, with a total length of 90317094bp, an average length of 903.68bp, and an N50 of 2001bp. The N50 of Transcript and Unigene were 1.47 and 2.21 times their average size, respectively, indicating high assembly integrity of the data, which can be used for subsequent analysis.

3.2 | Identification by DEGs

DEGs were identified and labeled by comparing AG, BG, and CG groups. The differences between AG, BG, and CG samples are shown in the Venn and volcano diagrams (Figure 2). In the comparison of AG versus CG, AG versus CG, and BG versus CG, there are 739 co-expression DEGs, 295, 2800, and 2060 Specific DEGs, respectively (Figure 2a). Compared with the AG group, 2369 DEGs were identified in the BG group, with 1346 upregulated, 1023 downregulated (Figure 2b,c), and 17,103 DEGs were placed in the CG group, with 8348 upregulated, 8755 downregulated (Figure 2b,d). Compared with the BG Group, 16,486 DEGs were identified in the CG group, with 8120 upregulated and 8366 downregulated (Figure 2b,e).

3.3 | GO annotation and enrichment analysis

GO is the international standard classification system for gene function, which divides DEGs into three categories: biological processes (BP), cellular components (CC), and molecular functions (MF). The directed acyclic graph (DAG) of these three categories and the GO enrichment histogram generated by classifying the rich GO entries are shown in Figure S1. The top five terms for the number of enriched DEGs in BPs, CCs and MFs in each comparison group are listed below.

In the AG versus BG comparison (Figure S1a and Table S1), DEGs in BPs were mainly enriched in the metabolic process (GO: 0008152, 703 genes), single-organism process (GO: 0044699, 551 genes), cellular process (GO: 0009987, 547 genes), biological regulation (GO: 0065007, 282 genes), and response to stimulus (GO: 0050896,

TABLE 3 Assembly result statistics.

Length range	Transcript	Unigene
200–300	12,6075 (13.77%)	37,514 (37.54%)
300–500	112,860 (12.32%)	24,489 (24.50%)
500–1000	182,922 (19.98%)	10,858 (10.86%)
1000–2000	279,333 (30.50%)	12,785 (12.79%)
2000+	214,560 (23.43%)	14,298 (14.31%)
Total number	915,750	99,944
Total length	1,264,342,025	90,317,094
N50 length	2033	2001
Mean length	1380.66	903.68

TABLE 2 Summary of RNA-seq data for mRNA.

Sample name	Read number	Base number	GC content (%)	≥Q30 (%)
AG1	20,655,120	6,184,700,152	42.71	93.94
AG2	20,970,369	6,279,362,032	43.47	93.75
AG3	20,730,511	6,207,578,484	43.39	92.93
BG1	20,999,338	6,286,559,408	43.32	93.74
BG2	20,862,349	6,245,083,188	43.73	93.58
BG3	21,925,055	6,562,503,388	43.70	93.81
CG1	19,619,650	5,870,716,890	43.50	92.99
CG2	20,518,995	6,139,118,844	43.73	93.74
CG3	20,346,158	6,088,909,376	43.71	93.13

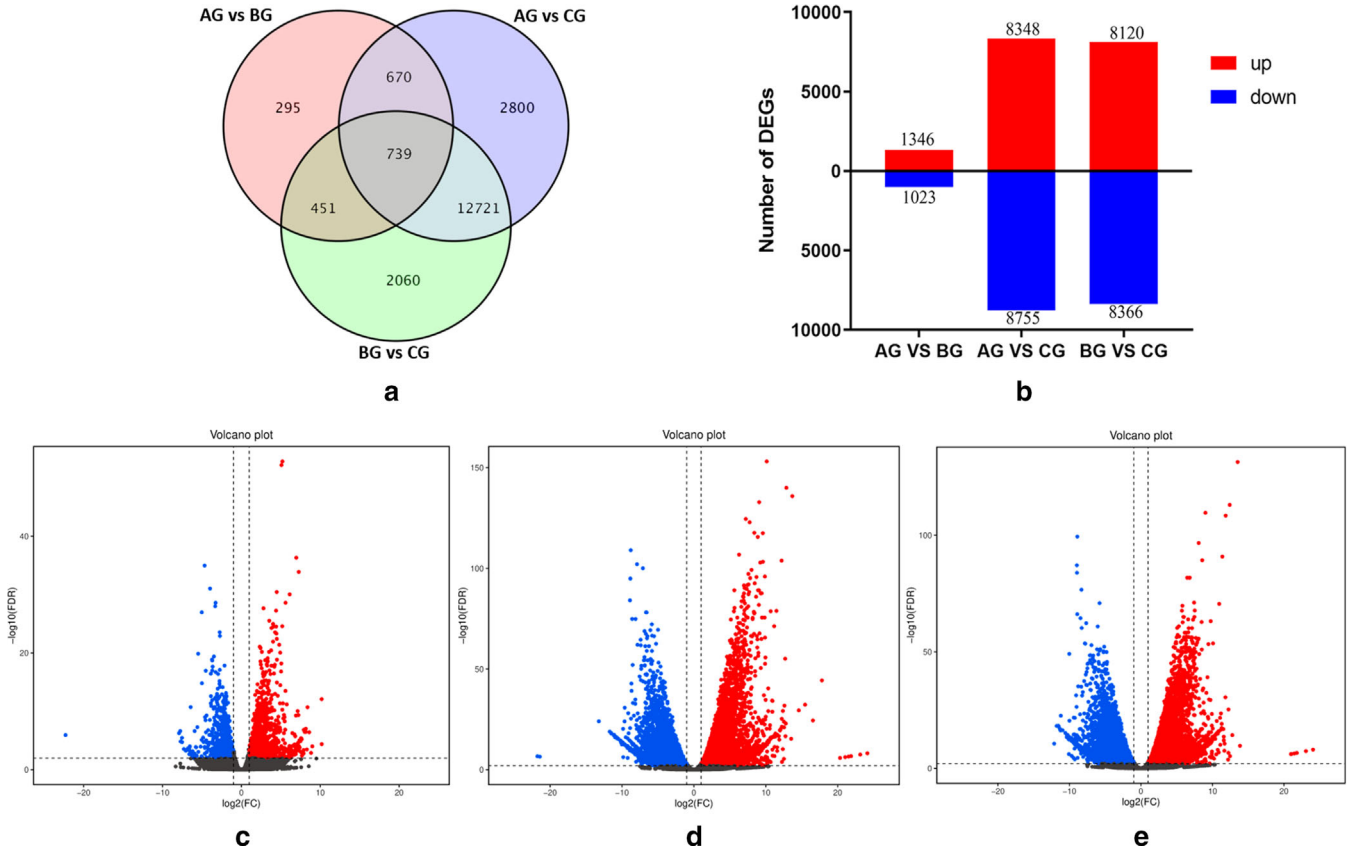

FIGURE 2 Expression profiling of genes in different tissues. (a) Venn diagram of differentially expressed genes (DEGs) in different tissues. (b) Numbers of upregulated and downregulated genes of different tissues. (c) Gene expression changes of AG versus BG. (d) Gene expression changes of AG versus CG. (e) Gene expression changes of BG versus CG. Red and blue represent DEGs upregulation and downregulation, respectively.

181 genes). DEGs in CCs were mainly enriched in membrane (GO: 0016020, 587 genes), membrane part (GO: 0044425, 539 genes), cell (GO: 0005623, 443 genes), cell part (GO: 0044464, 443 genes), and organelle (GO: 0043226, 321 genes). In MFs, DEGs were mainly enriched in catalytic activity (GO: 0003824, 807 genes), binding (GO: 0005488, 737 genes), nucleic acid binding transcription factor activity (GO: 0001071, 94 genes), transporter activity (GO: 0005215, 84 genes), and MF regulator (GO: 0098772, 28 genes).

In the AG versus CG comparison (Figure S1b and Table S2), DEGs in BPs were mainly enriched in metabolic process (GO: 0008152, 5693 genes), cellular process (GO: 0009987, 5414 genes), single-organism process (GO: 0044699, 3582 genes), biological regulation (GO: 0065007, 2132 genes), and localization (GO: 0051179, 1258 genes). In CCs, DEGs were mainly enriched in cell (GO: 0005623, 4151 genes), cell part (GO: 0044464, 4151 genes), organelle (GO: 0043226, 3307 genes), membrane (GO: 0016020, 3836 genes), and membrane part (GO: 0044425, 3400 genes). In MFs, DEGs were mainly enriched in binding (GO: 0005488, 6482 genes), catalytic activity (GO: 0003824, 5845 genes), transporter activity (GO: 0005215, 609 genes), nucleic acid binding transcription factor activity (GO: 0001071, 436 genes), and MF regulator (GO:0098772, 197 genes).

In the BG versus CG comparison (Figure S1C and Table S3), DEGs in BPs were mainly enriched in metabolic process (GO: 0008152, 5437 genes), cellular process (GO: 0009987, 5173 genes), single-organism process (GO: 0044699, 3349 genes), biological regulation (GO: 0065007, 1993 genes), and localization (GO: 0051179, 1217 genes). In CCs, DEGs were mainly enriched in cell (GO: 0005623, 4030 genes), cell part (GO: 0044464, 4030 genes), organelle (GO: 0043226, 3228 genes), membrane (GO: 0016020, 3631 genes), and membrane part (GO: 0044425, 3216 genes). In MFs, DEGs were mainly enriched in binding (GO: 0005488, 6141 genes), catalytic activity (GO: 0003824, 5483 genes), transporter activity (GO: 0005215, 592 genes), nucleic acid binding transcription factor activity (GO: 0001071 397 genes), and structural molecule activity (GO: 0005198, 250 genes).

3.4 | KEGG enrichment analysis

Taking pathway in the KEGG database as a unit, significant enrichment of pathways can identify the most critical biochemical metabolic pathways and signal transduction pathways involved in the response to the treatment of study. The top 20 KEGG pathways with the highest amount of DEGs enrichment were screened in different

groups. The results of DEGs in KEGG enrichment analysis were displayed by scatter plot (Figure 3). Compared with the AG, DEGs of the BG were mainly enriched in phenylpropanoid biosynthesis, plant hormone signal transduction, and MAPK signaling pathway-plant (Figure 3a and Table S4). Compared with AG and BG, the expression of DEGs related to plant hormone signal transduction and MAPK signaling pathway-plant was upregulated in the CG (Figure 3b,c, Tables S5 and S6). In the pathogenesis of GRS, phenylpropanoid biosynthesis, plant hormone signal transduction, and MAPK signal pathway-plant were enriched in more genes. Figures S2–S4 shows the specific pathway diagrams.

3.5 | GSEA analysis

In GSEA analysis, the KEGG pathway and the gene sets of BP, CC, and MF branches of GO were used as target gene sets, and log2FC scores of each different group were used as background gene sets to analyze the enrichment of target gene sets. Compared with the AG, the expression of genes related to lipid metabolic process, response to oxidative stress, cell wall, mitochondrial respiratory chain complex I, glycolysis/gluconeogenesis, α-linolenic acid metabolism, biosynthesis of unsaturated fatty acids, phenylpropanoid biosynthesis, fatty acid metabolism, monooxygenase activity, iron ion binding, UDP-glycosyltransferase activity, and oxidoreductase activity were upregulated in BG. In contrast, genes related to epithelium development were downregulated, as shown in Figure 4 and Table S7.

Between the AG versus CG, the upregulation of DEGs in the CG included pathways such as glucose metabolic process, ATP synthesis coupled proton transport, proteasome regulatory particle, oxidative phosphorylation, proteasome, and UDP-glycosyltransferase activity, as shown in Figure 5 and Table S8.

Compared with the BG, oxidative phosphorylation and proteasome-related DEGs expression were upregulated in the CG, while cortical microtubule cytoskeleton and amyloplast-related DEGs were downregulated, as shown in Figure 6 and Table S9.

3.6 | QRT-PCR validation of mRNA expression

Three upregulated and three downregulated DEGs were randomly selected from the transcriptome results for qRT-PCR analysis. The expression pattern of the qRT-PCR genes was consistent with the trend of RNA-seq data. As shown in Figure 7.

3.7 | Determination of $O_2^{\bullet-}$, H2O2, and MDA contents

The contents of $O_2^{\bullet-}$, H_2O_2, and MDA in BG and CG were higher than those in the AG, among which the contents of $O_2^{\bullet-}$ and H_2O_2 were the highest in the BG group, and the contents of MDA were the highest in CG. As shown in Figure 8.

3.8 | Validation of ROS-induced GRS

As shown in Figure 9, ginseng in the $Na_2S_2O_4$-stress group showed irregular red rust-colored scars on the epidermis after treatment, consistent with the appearance characterization of GRS.

4 | ANALYSIS AND DISCUSSION

4.1 | GO enrichment analysis

The expression of DEGs in each group is shown in Figure 2. Compared with AG and BG, CG contains more DEGs, indicating significant changes in transcription levels before and after GRS. Compared with the two pairs of AG versus CG and BG versus CG, fewer DEGs were identified between AG and BG, but it was still as high as 2349 genes, which was not negligible. Figure S1 shows the order of the GO terms ranked by the quantity of DEG enrichment, in which the metabolic process ranked first in the BPs of the three comparison groups, indicating that metabolism changes accompany the entire occurrence process of GRS. The order of GO terms of AG versus CG and BG versus CG in BPs, CCs, and MFs was almost entirely consistent (Figure S1a,b), and the number of co-expressed DEGs reached 13,460 (Figure 2a), with a high degree of similarity. The specific DEGs in the two comparison groups were as high as 2800 and 2060 genes, respectively (Figure 2a). However, most of them were located downstream of the reaction pathway after identification. For example, GH3 is the downstream gene of the plant hormone signal transduction pathway (Jain et al., 2006); DWF1 is a downstream gene of the steroid biosynthesis pathway (Choe et al., 1999). The presence of so many specific DEGs may be due to metabolic disorders in the rusty plaque tissue. Unlike AG versus CG and BG versus CG, GO terms strongly correlated with the stress response, such as response to stimulus, membrane, and catalytic activity, ranked first in the AG versus BG comparison. Only 295 specific DEGs exist in the AG versus CG comparison, but most are upstream genes involved in stress response pathways. For instance, ACOX is the upstream gene of the peroxisome pathway, which is closely associated with oxidative stress in plants (Vasilev et al., 2022). For the rusty ginseng, DEGs in CG were also the marker genes of GRS, but it was only the result of GRS, not the cause. Although no characteristics of GRS were found in BG sampling sites, the above results indicated that ginseng tissues in the BG group had an initial physiological response to stress. Therefore, the DEGs in AG versus BG are the focus of the subsequent research on the genesis of GRS.

4.2 | KEGG enrichment analysis

Figure 3 shows that DEGs in KEGG enrichment were mainly concentrated in phenylpropanoid biosynthesis, plant hormone signal transduction, and MAPK signaling pathway.

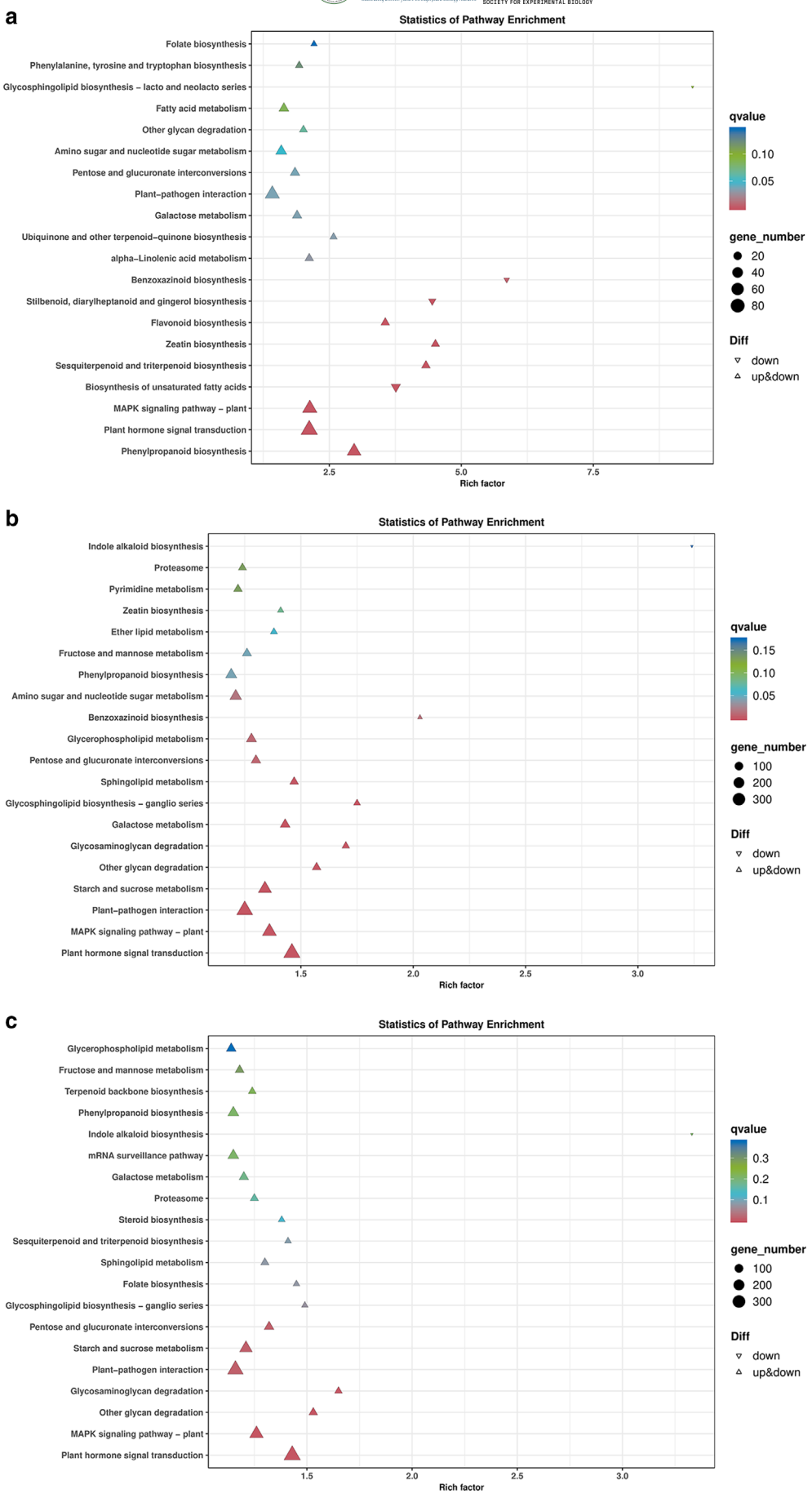

FIGURE 3 Scatter plot of Kyoto Encyclopedia of Genes and Genome (KEGG) pathway enrichment of differentially expressed genes (DEGs). (a) Pathways of DEGs in AG and BG. (b) Pathways of DEGs in AG and CG. (c) Pathways of DEGs in BG and CG. The color and size of the scatter represent the *q*-value and the number of enriched genes, respectively. The smaller the *q*-value, the more enriched genes, indicating that enrichment results are more reliable.

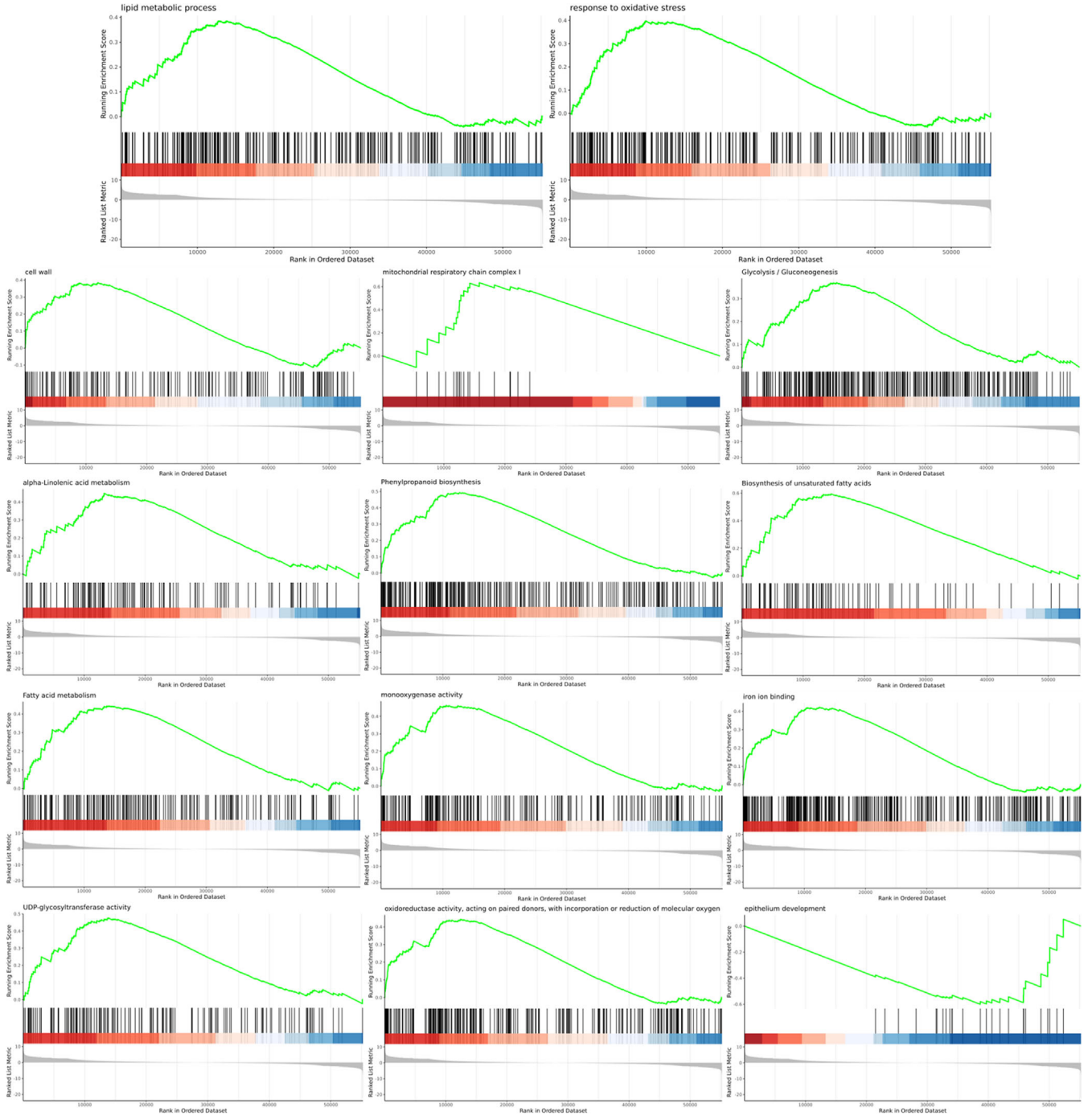

FIGURE 4 AG and BG comparison analysis based on gene set enrichment analysis (GSEA). The green lines represent the enrichment score (ES). The black lines represent genes examined gene set. The absolute values of the ES peak in the red and blue regions represent the gene set upregulation and downregulation, respectively.

4.2.1 | Phenylpropanoid biosynthesis

Phenylpropanoid is the basic unit in the formation of lignin, a highly branched polymer of phenylpropanoid compounds, which enhances the stability of the cell wall structure and provides the plant's first defensive barrier (Pesquet et al., 2019; Shi et al., 2022). ROS can regulate lignin synthase activity, promote lignin accumulation, and improve plants' antioxidant capacity (Chenyu et al., 2018; Zheng et al., 2021). Compared with the AG, the number of upregulated phenylpropanoid biosynthetic pathway genes in BG ranked first (Figure 3a), among which 4-coumarate-CoA ligase (4CL), ferulate 5-hydroxylase (F5H), and shikimate O-hydroxycinnamoyl transferase (HCT), are essential enzyme-related genes in lignin synthesis (Figure S2), and ROS may cause these changes. Compared with the AG, the DEGs of this pathway in the CG were insignificant (Figure 3b,c), possibly due to the severe damage to the cell wall and the weakening of related metabolism in the CG.

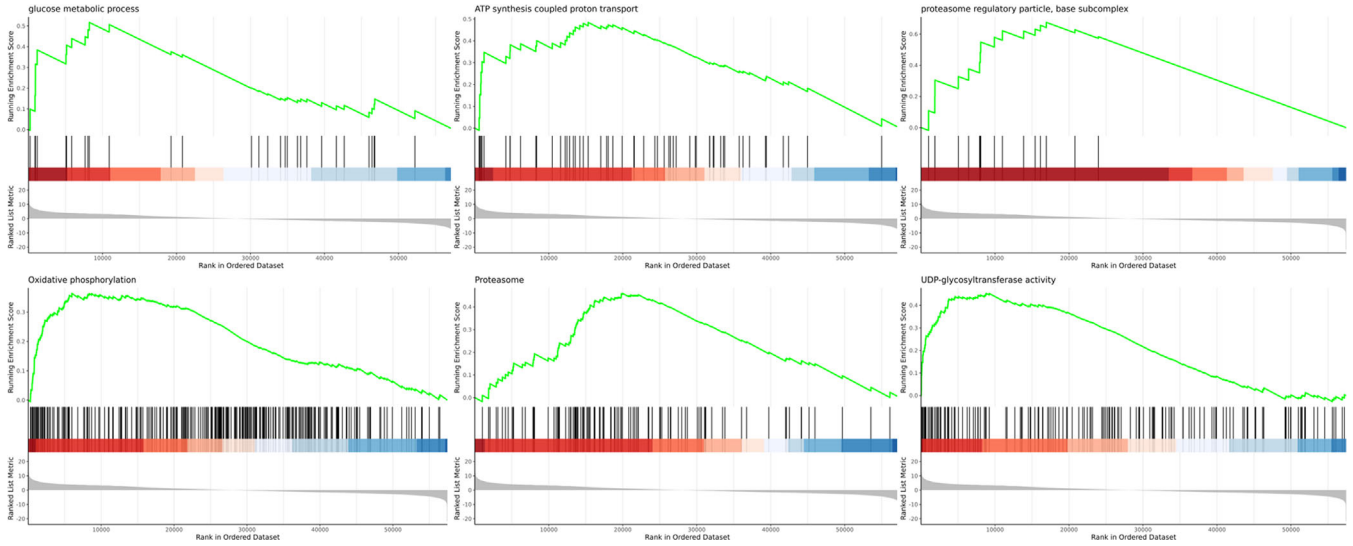

FIGURE 5 AG and CG comparison analysis based on gene set enrichment analysis (GSEA). The green lines represent the enrichment score (ES). The black lines represent genes examined gene set. The absolute value of the ES peak in the red region represents the gene set upregulation.

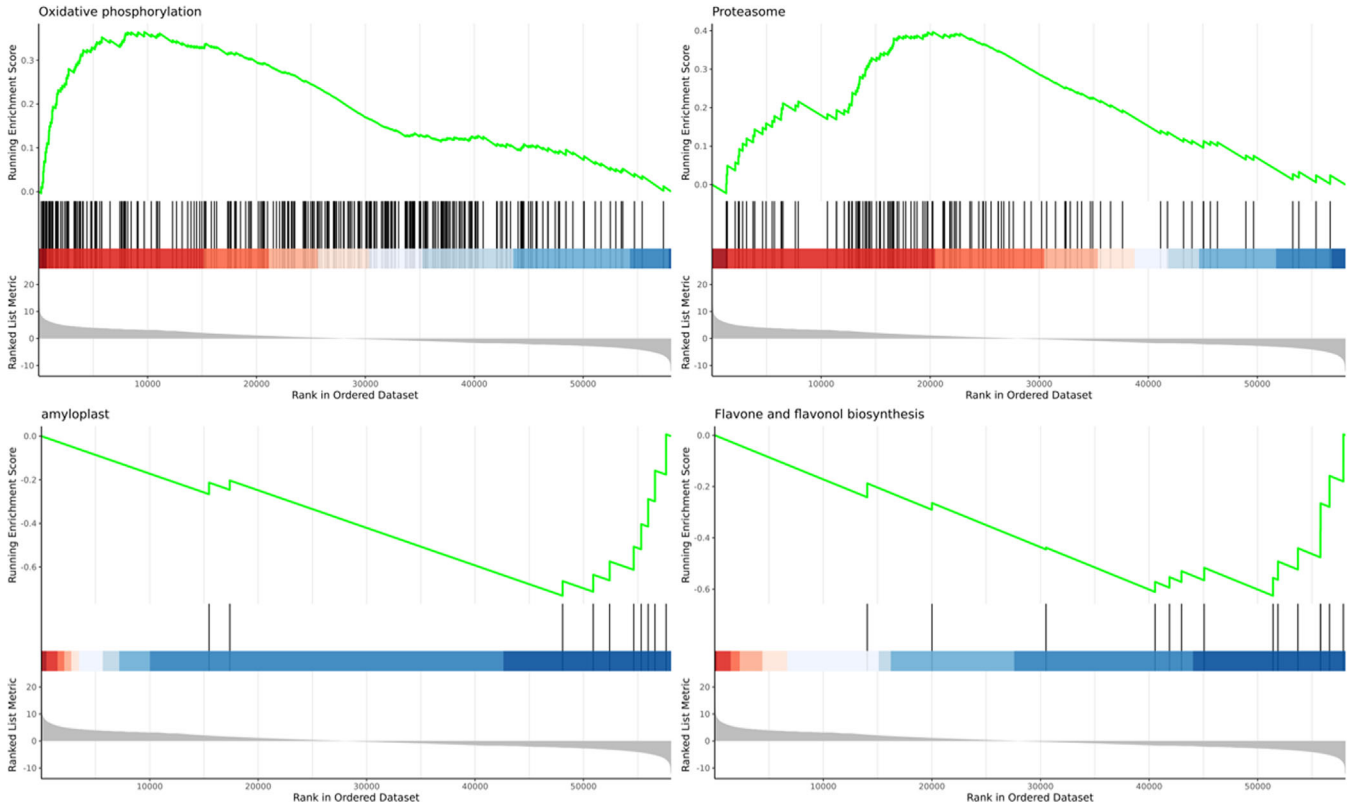

FIGURE 6 BG and CG comparison analysis based on gene set enrichment analysis (GSEA). The green lines represent the enrichment score (ES). The black lines represent genes examined gene set. The absolute value of the ES peak in the red region represents the gene set upregulation.

4.2.2 | Plant hormone signal transduction

Plant hormones are active substances that regulate physiological responses in plants and are induced by plant cells receiving specific environmental signals to regulate cell division and elongation, tissue and organ differentiation, flowering and fruit set, maturation and senescence, and dormancy and germination.

Plant growth and development retardation under stress conditions are inevitably related to hormones (Verma et al., 2016). Figure S3 shows that abscisic acid (ABA), salicylic acid (SA),

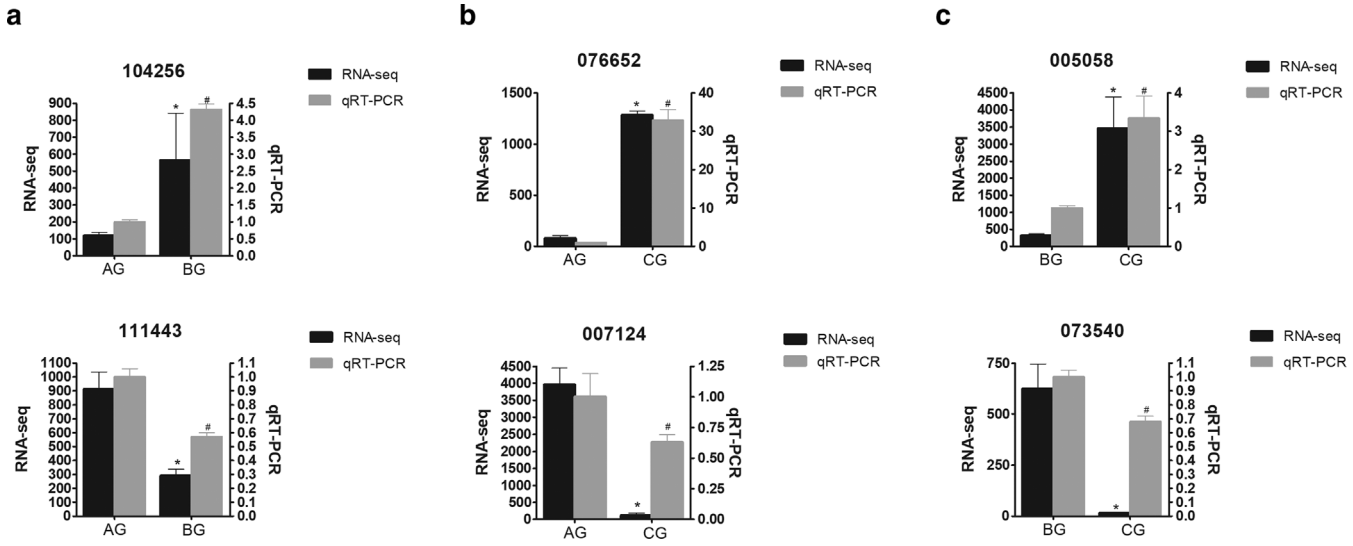

FIGURE 7 qRT-PCR verification of differentially expressed genes (DEGs). (a) DEGs in AG versus BG. (b) DEGs in AG versus CG. (c) DEGs in BG versus CG. *:p<.05 in RNA-seq comparison group; #:p<.05 in qRT-PCR comparison group.

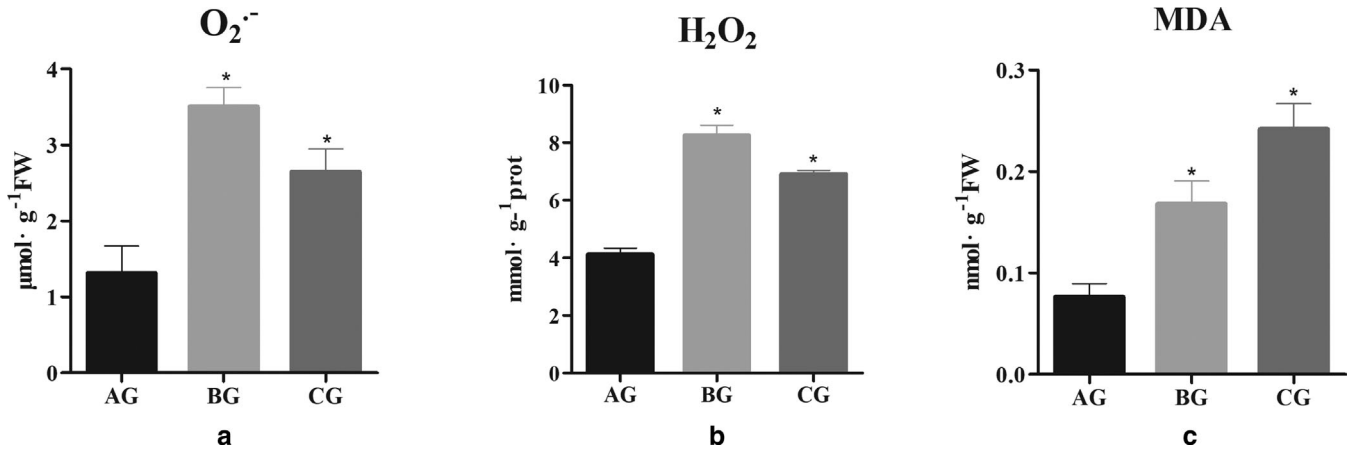

FIGURE 8 Changes of $O_2^{\bullet-}$, H_2O_2, and MDA at different stages of Ginseng rusty root symptoms (GRS). *: p<.05 versus AG.

methyl-jasmonate (MeJA), and ethylene (ET)-related regulatory factors PYR/P4YL, TGA, COI1, and ETR were all upregulated after stress, which is consistent with the results of Bian et al. (Bian et al., 2021). It has been shown that ROS can affect the biosynthesis of hormones such as SA and ET (Dempsey & Klessig, 1995; Ievinsh & Tillberg, 1995). In addition, as the most critical stress-regulatory hormone in plants, ABA can also interact with ROS in response to stress (He et al., 2022; Kun et al., 2016; Liu et al., 2010).

4.2.3 | MAPK signaling pathway

MAPK signaling pathway plays a vital role in cell growth, differentiation, and adaptation to environmental stress. There is a feedback loop of mutual regulation between ROS and MAPKs: ROS can activate MAPKs under stress conditions and are further regulated by MAPK to maintain homeostasis (Jalmi & Sinha, 2015). Figure S4 shows the changes in the MAPK signaling pathway after environmental stress. Respiratory burst oxidase homolog D (RbohD), a ROS-related enzyme located on the cell membrane, was activated in the BG, promoting ROS accumulation (Miller et al., 2009). Compared with the AG, the BG directly upregulates the expression of genes related to upstream protein MPK3/6 and then upregulates the expression of genes associated with WRKY22/29. WRKY22/29 not only acts on the early defense response to pathogens but also promotes excessive production of H_2O_2 (Kovtun et al., 2000). Multiple plant hormone receptors acting upstream of MAPK were also identified. Compared with the AG, abscisic acid receptor PYR/PYL-related genes were upregulated in the BG and regulated the adaptation of *P. ginseng* to stress (Hu et al., 2012). In this study, the upregulated MPK 3/6 and ACS6 in the BG group would promote ethylene biosynthesis, further leading to the upregulation of PDF1.2 and ChiB expression, ultimately

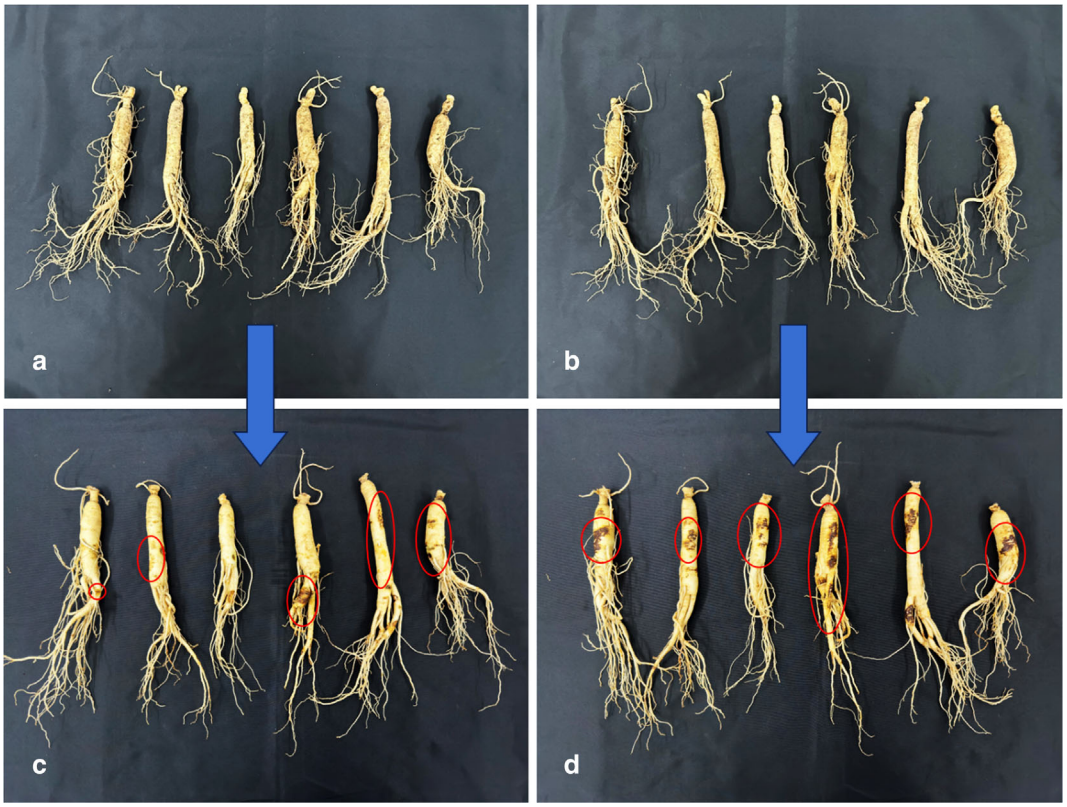

FIGURE 9 Verification of reactive oxygen species (ROS)-induced Ginseng rusty root symptoms (GRS). (a,b) Ginseng before $Na_2S_2O_4$ induction. (c,d) Ginseng after $Na_2S_2O_4$ induction; red circle: red rust-like patches.

regulating the defense response to stress (Ju et al., 2012; Liu & Zhang, 2004; Solano et al., 1998).

In addition, Figure S4 also shows that the downstream gene MYC2 of the JA pathway branch was upregulated, which would further activate VSP2 and antagonize the damage caused by ROS (Howlader et al., 2020; Vos et al., 2013).

4.3 | GSEA analysis

The analysis of GSEA shows that compared with the AG, the expression of genes related to epithelium development (25 genes) was downregulated. The expression of genes related to the cell wall (180 genes) was upregulated in the BG, indicating that the physiological state of the plants had changed before the onset of GRS (Figure 4 and Table S7). The proteasome, which maintains cell stability and regulate stress response, is an essential regulatory complex in plant response to stress (Xu & Xue, 2019). Compared with the AG, the expressions of genes related to the proteasome (116 genes) and proteasome regulatory particle (16 genes) were upregulated in the CG, further indicating that the occurrence of GRS was related to stress (Figure 5 and Table S8).

ROS is the product of organisms under stress, and its content is bound to increase under unfavorable conditions (Caverzan et al., 2016). Mitochondria are the main organelles of ROS production in ginseng root. Electron leakage of the respiratory chain enzyme complex I and III results in the single-electron reduction of molecular oxygen to $O_2^{\bullet-}$. At the same time, excessive production of ATP can also cooperatively produce a large number of ROS (Jardim-Messeder et al., 2022). Figures 4–6 and Tables S7–S9 show that the genes related to mitochondrial respiratory chain complex I (19 genes), oxidative phosphorylation (295 genes), and ATP synthesis coupled proton transport (57 genes) were upregulated with the occurrence of GRS. Excessive ROS can cause lipid peroxidation damage to the cell membrane, but plants can protect cells by maintaining membrane fluidity and integrity. α-linolenic acid is the primary unsaturated fatty acid in membranes and can play an essential role in lipid metabolism and maintaining the normal function of cell membrane under stress (Liu et al., 2021). The glycolysis process is the prerequisite for synthesizing fatty acids, followed by the formation of various lipids in the cytoplasm and endoplasmic membrane through the elongation and desaturation of fatty acid carbon chains (Plaxton, 1996). The expression of lipid metabolic process (255 genes), α-linolenic acid metabolism (131 genes), glycolysis/gluconeogenesis (336 genes), biosynthesis of unsaturated fatty acids (88 genes), and fatty acid metabolism (214 genes) in the BG were also upregulated compared with AG, as shown in Figure 4 and Table S7. With this, resistance of ginseng to stress was enhanced.

Plants always adopt a series of protective measures to cope with the ROS explosion caused by environmental stress, among which the

enzymatic clearance system is the primary pathway for plants to remove ROS. Antioxidant enzymes begin to function when plants are subjected to environmental stress (Dvořák et al., 2021). Compared with the AG, the expression of antioxidant-related genes, such as oxidative stress (238 genes) and oxidoreductase activity (272 genes), was upregulated in the BG (Figure 4 and Table S7). With the aggravation of GRS (Figure 5 and Table S8), the expression of DEGs related to oxidative phosphorylation (294 genes) in the CG was upregulated, indicating that a large number of ROS were produced in GRS, and the antioxidant oxidase system was also activated, with a positive correlation with the environmental stress.

4.4 | GRS and secondary metabolites

Plants cannot avoid stress by moving and inevitably produce excessive ROS under unfavorable conditions. Due to the damage that ROS causes to proteins, it is impossible for plants to eliminate redundant ROS by antioxidant enzymes alone, and plants have therefore evolved unique secondary metabolites to reduce the damage caused by ROS (Cao et al., 2022; Huimin et al., 2019). Ginsenosides, a triterpenoid component, are ginseng's most important secondary metabolites. Compared with the AG, the expression of genes related to ginsenoside synthesis, such as sesquiterpenoid and triterpenoid biosynthesis (21 genes), were upregulated in the BG (Figure 3a and Table S4). GSEA analysis results show (Figures 4 and 5 and Tables S7 and S8) that UDP-glycosyltransferase activities-related genes (AG versus BG: 164 genes, BG versus CG:178 genes)were upregulated, likely promoting ginsenoside synthesis and modification. Additionally, the expression of phenylpropanoid biosynthesis (319 genes) and monooxygenase (223 genes), which are involved in the biosynthesis of various secondary metabolites (Guo et al., 2016; Zhao et al., 2018) were also upregulated (Figure 4 and Table S7). It has been shown that ROS can induce the biosynthesis of secondary metabolites and that secondary metabolites increase with the increasing ROS contents over a range (Xiao et al., 2009). The above result indicates that these changes are also related to ROS.

4.5 | Etiological analysis of GRS

Previous work showed that bacterial species diversity in the rhizosphere soil of GRS was higher (Bian et al., 2020). However, there was no significant correlation between the degree of GRS and the abundance of bacteria in the rhizosphere of ginseng (Wang, Sun, Xu, Ma, Li, Shao, Guan, Liu, Liu, & Zhang, 2019). It has been shown that GRS is related to the synthesis of phenolic compounds, and these phenolic compounds are also induced by ROS produced in plants under stress (Gill & Tuteja, 2010; Naikoo et al., 2019). A large amount of heavy metal ions such as Al^{3+} and Fe^{3+} were detected in the GRS epidermis (Yang et al., 1997; Zhao & Li, 1998). Excessive soil moisture will cause poor soil aeration, anaerobic bacteria that proliferate rapidly, and increased soil acidity (Van Breemen et al., 1983), resulting in an increase of Al^{3+}. Under acidic, anaerobic conditions, Fe^{2+} content increases and is quickly oxidized by ROS efflux from the cells to red Fe^{3+}, which is deposited in the ginseng epidermis. In the conversion of Fe^{2+} to Fe^{3+}, more of the highly destructive ·OH is produced, causing oxidative stress and damaging cell membrane structure (Kehrer, 2000). Moreover, a variety of complex organic complexes containing aluminum and iron were detected on the surface of GRS, which may be a product of cell membrane disruption by ROS (Zhao, 1998), and during the occurrence of GRS, the expression of genes related to iron ion binding (355 genes) was upregulated (Figure 4 and Table S7).

To verify the hypothesis that ROS caused GRS, the contents of $O_2^{\bullet-}$, H_2O_2, and MDA were detected. The content of $O_2^{\bullet-}$ and H_2O_2 represents the level of ROS, MDA can be used to evaluate the extent of lipid peroxidation of membrane and damage to the membrane system, and is a product of ROS damage to the cell membrane (Liu et al., 2015). The contents of $O_2^{\bullet-}$, H_2O_2, and MDA in the BG and CG are higher than those in the AG, among which the contents of $O_2^{\bullet-}$ and H_2O_2 in BG are the highest, while the contents of MDA in the CG are the highest, as shown in Figure 8.

4.6 | Validation of ROS-induced GRS

The results of the above studies showed that ROS is the underlying cause of GRS production. To verify the hypothesis, $Na_2S_2O_4$ solution was chosen as the $O_2^{\bullet-}$ donor for the induction test of ginseng to stimulate the production of excess ROS under environmental stresses. As shown in Figure 9, ginseng plants treated with $Na_2S_2O_4$ showed prominent GRS characteristics, which showed irregular patches of different shades of color from red to red-brown. Induction experiments successfully demonstrated that ROS produced under environmental stress was the essential cause of GRS.

5 | CONCLUSION

During the occurrence of GRS, the genes associated with plant stress resistance respond rapidly. The hypoxic environment developed in acidic waterlogged soils leads to an overproduction of ROS in the roots, which alters the expression and pathway of defense-related genes to cope with the outbreak of ROS. In the meantime, Fe^{2+} around the root zone is reduced to red Fe^{3+} by ROS and deposited, giving a reddish-brown phenotype. The results of this study provide a basis for future prevention and treatment of GRS.

AUTHOR CONTRIBUTIONS

Study conception and design: Pengcheng Yu and Xiangcai Meng; data collection: Xiaowen Song, Wei Zhang and Yao Yao; analysis and interpretation of results: Junling Ren, Liyang Wang, Wenfei Liu, and Zhaoping Meng; draft manuscript preparation: Pengcheng Yu and Xiangcai Meng. All authors reviewed the results and approved the final version of the manuscript.

ACKNOWLEDGMENTS

The authors gratefully acknowledge the financial support by the National Natural Science Foundation of China under Grant number 20012210001, as well as the University Nursing Program for Young Scholars with Creative Talents in Heilongjiang Province under grant number UNPYSCT-2020224.

CONFLICT OF INTEREST STATEMENT

The authors declare that they have no conflicts of interest to report regarding the present study.

PEER REVIEW

The peer review history for this article is available in the Supporting Information for this article.

DATA AVAILABILITY STATEMENT

All data generated or analyzed during this study are included in this published article. Transcriptome data are available from NCBI database under BioProject ID PRJNA993718.

ETHICS STATEMENT

Not applicable.

ORCID

Pengcheng Yu https://orcid.org/0000-0002-3793-4013

Xiangcai Meng https://orcid.org/0000-0003-1868-4810

REFERENCES

Bian, X., Xiao, S., Zhao, Y., Xu, Y., Yang, H., & Zhang, L. (2020). Comparative analysis of rhizosphere soil physiochemical characteristics and microbial communities between rusty and healthy ginseng root. *Scientific Reports*, *10*(1), 15756. https://doi.org/10.1038/s41598-020-71024-8

Bian, X., Zhao, Y., Xiao, S., Yang, H., Han, Y., & Zhang, L. (2021). Metabolome and transcriptome analysis reveals the molecular profiles underlying the ginseng response to rusty root symptoms. *BMC Plant Biology*, *21*(1), 215. https://doi.org/10.1186/s12870-021-03001-w

Cao, S., Shi, L., Shen, Y., He, L., & Meng, X. (2022). Ecological roles of secondary metabolites of Saposhnikovia divaricata in adaptation to drought stress. *PeerJ*, *10*, e14336. https://doi.org/10.7717/peerj.14336

Caverzan, A., Casassola, A., & Brammer, S. P. (2016). Reactive oxygen species and antioxidant enzymes involved in plant tolerance to stress. In *Abiotic and biotic stress in plants-recent advances and future perspectives* (1st ed., Vol. 17) (pp. 463–480). IntechOpen. https://doi.org/10.5772/61368

Chenyu, Y., Yingbo, L., Dewen, Q., Hongmei, Z., Jingjing, Y., & Xiufen, Y. (2018). Lignin metabolism involves Botrytis cinerea BcGs1-induced defense response in tomato. *BMC Plant Biology*, *18*(1), 1–15.

Choe, S., Dilkes, B. P., Gregory, B. D., Ross, A. S., Yuan, H., & Noguchi, T. (1999). The arabidopsis dwarf1 mutant is defective in the conversion of 24-methylenecholesterol to campesterol in brassinosteroid biosynthesis. *Plant Physiology*, *119*(3), 897–907. https://doi.org/10.1104/pp.119.3.897

Dempsey, D., & Klessig, D. (1995). Signals in plant disease resistance. *Bulletin de l'Institut Pasteur*, *93*(3), 167–186. https://doi.org/10.1016/0020-2452(96)81488-6

Dvořák, P., Krasylenko, Y., Zeiner, A., Šamaj, J., & Takáč, T. (2021). Signaling toward reactive oxygen species-scavenging enzymes in plants. *Frontiers in Plant Science*, *11*, 618835. https://doi.org/10.3389/fpls.2020.618835

Fan, W. X., Zhan, Z. L., Hou, F. J., & Zheng, Y. G. (2021). Research progress on chemical constituents and pharmacological activities of ginseng radix et Rhizoma Rubra. *Natural Product Research and Development*, *33*(1), 137.

Farh, E. A., Kim, Y. J., Sukweenadhi, J., Singh, P., & Yang, D. C. (2017). Aluminium resistant, plant growth promoting bacteria induce overexpression of Aluminium stress related genes in Arabidopsis thaliana and increase the ginseng tolerance against Aluminium stress. *Microbiological Research*, *200*, 45–52. https://doi.org/10.1016/j.micres.2017.04.004

Garg, N., & Manchanda, G. (2009). ROS generation in plants: Boon or bane? *Plant Biosystems*, *143*(1), 81–96. https://doi.org/10.1080/11263500802633626

Gill, S. S., & Tuteja, N. (2010). Reactive oxygen species and antioxidant machinery in abiotic stress tolerance in crop plants. *Plant Physiology and Biochemistry*, *48*(12), 909–930. https://doi.org/10.1016/j.plaphy.2010.08.016

Grabherr, M. G., Haas, B. J., Yassour, M., Levin, J. Z., Thompson, D. A., Amit, I., Adiconis, X., Fan, L., Raychowdhury, R., & Zeng, Q. (2011). Full-length transcriptome assembly from RNA-Seq data without a reference genome. *Nature Biotechnology*, *29*(7), 644–652. https://doi.org/10.1038/nbt.1883

Guan, Y., Fan, J., Sun, C., Quan, J., Zhang, G., & Guo, N. (2022). Differences in the chemical composition of Panax ginseng roots infected with red rust. *Journal of Ethnopharmacology*, *283*, 114610. https://doi.org/10.1016/j.jep.2021.114610

Guo, J., Ma, X., Cai, Y., Ma, Y., Zhan, Z., Zhou, Y. J., Liu, W., Guan, M., Yang, J., & Cui, G. (2016). Cytochrome P450 promiscuity leads to a bifurcating biosynthetic pathway for tanshinones. *The New Phytologist*, *210*(2), 525–534. https://doi.org/10.1111/nph.13790

He, Q. Y., Jin, J. F., Lou, H. Q., Dang, F. F., Xu, J. M., Zheng, S. J., & Yang, J. L. (2022). Abscisic acid-dependent PMT1 expression regulates salt tolerance by alleviating abscisic acid-mediated reactive oxygen species production in Arabidopsis. *Journal of Integrative Plant Biology*, *64*(9), 18–1820. https://doi.org/10.1111/jipb.13326

Howlader, P., Bose, S. K., Jia, X., Zhang, C., Wang, W., & Yin, H. (2020). Oligogalacturonides induce resistance in Arabidopsis thaliana by triggering salicylic acid and jasmonic acid pathways against Pst DC3000. *International Journal of Biological Macromolecules*, *164*, 4054–4064. https://doi.org/10.1016/j.ijbiomac.2020.09.026

Hu, S., Wang, F. Z., Liu, Z. N., Liu, Y. P., & Yu, X. L. (2012). ABA signaling mediated by PYR/PYL/RCAR in plants. *Yi Chuan= Hereditas 2012*, *34*(5), 560–572. https://doi.org/10.3724/SP.J.1005.2012.00560

Huimin, G., Jiahui, W., Huiru, G., & Xiangcai, M. (2019). High-temperature condition increases lignanoid biosynthesis of Schisandra chinensis seeds via reactive oxygen species. *Pharmacognosy Research*, *11*(1), 72. https://doi.org/10.4103/pr.pr_42_18

Hung, J. H., Yang, T. H., Hu, Z., Weng, Z., & DeLisi, C. (2012). Gene set enrichment analysis: Performance evaluation and usage guidelines. *Briefings in Bioinformatics*, *13*(3), 281–291. https://doi.org/10.1093/bib/bbr049

Ievinsh, G., & Tillberg, E. (1995). Stress-induced ethylene biosynthesis in pine needles: A search for the putative 1-aminocyclopropane-l-carboxylic acid-independent pathway. *Journal of Plant Physiology*, *145*(3), 308–314. https://doi.org/10.1016/S0176-1617(11)81895-X

Jain, M., Kaur, N., Tyagi, A. K., & Khurana, J. P. (2006). The auxin-responsive gh3 gene family in rice (oryza sativa). *Functional & Integrative Genomics*, *6*(1), 36–46. https://doi.org/10.1007/s10142-005-0142-5

Jalmi, S. K., & Sinha, A. K. (2015). ROS mediated MAPK signaling in abiotic and biotic stress-striking similarities and differences. *Frontiers in Plant Science*, *6*, 769. https://doi.org/10.3389/fpls.2015.00769

Jardim-Messeder, D., Margis-Pinheiro, M., & Sachetto-Martins, G. (2022). Salicylic acid and adenine nucleotides regulate the electron transport system and ROS production in plant mitochondria. *Biochimica et Biophysica Acta-Bioenergetics*, *1863*(6), 148559. https://doi.org/10.1016/j.bbabio.2022.148559

Ju, C., Yoon, G. M., Shemansky, J. M., Lin, D. Y., Ying, Z. I., Chang, J., Garrett, W. M., Kessenbrock, M., Groth, G., & Tucker, M. L. (2012). CTR1 phosphorylates the central regulator EIN2 to control ethylene hormone signaling from the ER membrane to the nucleus in Arabidopsis. *Proceedings of the National Academy of Sciences*, *109*(47), 19486–19491. https://doi.org/10.1073/pnas.1214848109

Kehrer, J. P. (2000). The Haber–Weiss reaction and mechanisms of toxicity. *Toxicology*, *149*(1), 43–50. https://doi.org/10.1016/S0300-483X(00)00231-6

Kovtun, Y., Chiu, W. L., Tena, G., & Sheen, J. (2000). Functional analysis of oxidative stress-activated mitogen-activated protein kinase cascade in plants. *Proceedings of the National Academy of Sciences*, *97*(6), 2940–2945. https://doi.org/10.1073/pnas.97.6.2940

Kun, L., Yuli, D., & Yuchen, M. (2016). Institute of plant stress future challenges in understanding ROS in plant responses to abiotic stress. *Science China. Life Sciences*, *59*(12), 2. (In Chinese)

Lee, C., Kim, K., Lee, J., Kim, S., Ryu, D., Choi, J., & An, G. (2011). Enzymes hydrolyzing structural components and ferrous ion cause rusty-root symptom on ginseng (Panax ginseng). *Journal of Microbiology and Biotechnology*, *21*(2), 192–196. https://doi.org/10.4014/jmb.1008.08010

Li, S., Wang, P., Yang, W., Zhao, C., Zhang, L., Zhang, J., Qin, Y., Xu, H., & Huang, L. (2021). Characterization of the components and pharmacological effects of mountain-cultivated ginseng and garden ginseng based on the integrative pharmacology strategy. *Frontiers in Pharmacology*, *12*, 659954. https://doi.org/10.3389/fphar.2021.659954

Li, Z., Tian, S., Sun, Y., Guo, S., & Liu, Z. (1999). Relationship between the genesis of ginseng rust spots and soil ecological conditions. *Acta Ecologica Sinica*, *19*(6), 864–869. (In Chinese)

Liu, H., Zhang, G., Wang, J., Qingsong, B. A., & Chen, L. (2015). The relationship between male sterility and membrane lipid peroxidation and antioxidant enzymes in wheat (Triticum aestivum L.). *Turkish Journal of Field Crop*, *20*(2), 179–187. https://doi.org/10.17557/tjfc.34046

Liu, J., Zhao, Y., & Liu, B. (1998). A study on the anatomical and morphological characteristics of the ginseng roots infected by the red root disease. *Acta Phytopathologica Sinica*, *28*(01), 73. (In Chinese)

Liu, W., Zhang, R., Xiang, C., Zhang, R., Wang, Q., Wang, T., Li, X., Lu, X., Gao, S., & Liu, Z. (2021). Transcriptomic and physiological analysis reveal that α-linolenic acid biosynthesis responds to early chilling tolerance in pumpkin rootstock varieties. *Frontiers in Plant Science*, *12*, 669565. https://doi.org/10.3389/fpls.2021.669565

Liu, Y., Ye, N., Liu, R., Chen, X., & Zhang, J. (2010). H2O2 mediates the regulation of ABA catabolism and GA biosynthesis in Arabidopsis seed dormancy and germination. *Journal of Experimental Botany*, *61*(11), 2979–2990. https://doi.org/10.1093/jxb/erq125

Liu, Y., & Zhang, S. (2004). Phosphorylation of 1-aminocyclopropane-1-carboxylic acid synthase by MPK6, a stress-responsive mitogen-activated protein kinase, induces ethylene biosynthesis in Arabidopsis. *Plant Cell*, *16*(12), 3386–3399. https://doi.org/10.1105/tpc.104.026609

Love, M. I., Huber, W., & Anders, S. (2014). Moderated estimation of fold change and dispersion for RNA-seq data with DESeq2. *Genome Biology*, *15*(12), 550. https://doi.org/10.1186/s13059-014-0550-8

Lowe, R., Shirley, N., Bleackley, M., Dolan, S., & Shafee, T. (2017). Transcriptomics technologies. *PLoS Computational Biology*, *13*(5), e1005457. https://doi.org/10.1371/journal.pcbi.1005457

Mansoor, S., Ali Wani, O., Lone, J. K., Manhas, S., Kour, N., Alam, P., & Ahmad, P. (2022). Reactive oxygen species in plants: From source to sink. *Antioxidants-Basel*, *11*(2), 225. https://doi.org/10.3390/antiox11020225

McGettigan, P. A. (2013). Transcriptomics in the RNA-seq era. *Current Opinion in Chemical Biology*, *17*(1), 4–11. https://doi.org/10.1016/j.cbpa.2012.12.008

Miller, G., Schlauch, K., Tam, R., Cortes, D., Torres, M. A., Shulaev, V., Dangl, J. L., & Mittler, R. (2009). The plant NADPH oxidase RBOHD mediates rapid systemic signaling in response to diverse stimuli. *Science Signaling*, *2*(84), ra45-ra45. https://doi.org/10.1126/scisignal.2000448

Naikoo, M. I., Dar, M. I., Raghib, F., Jaleel, H., Ahmad, B., Raina, A., Khan, F. A., & Naushin, F. (2019). Role and regulation of plants Phenolics in abiotic stress tolerance. *Plant Signaling Molecules*, *2019*, 157–168. https://doi.org/10.1016/B978-0-12-816451-8.00009-5

Pesquet, E., Wagner, A., & Grabber, J. H. (2019). Cell culture systems: Invaluable tools to investigate lignin formation and cell wall properties. *Current Opinion in Biotechnology*, *56*, 215–222. https://doi.org/10.1016/j.copbio.2019.02.001

Plaxton, W. C. (1996). The organization and regulation of plant glycolysis. *Annual Review of Plant Biology*, *47*(1), 185–214. https://doi.org/10.1146/annurev.arplant.47.1.185

Proctor, J., & Bailey, W. (1987). Ginseng: Industry, botany, and culture. *Horticultural Reviews*, *9*, 187–236. https://doi.org/10.1002/9781118060827.ch6

Shi, J., Yan, X., Sun, T., Shen, Y., Shi, Q., Wang, W., Bao, M., Luo, H., Nian, F., & Ning, G. (2022). Homeostatic regulation of flavonoid and lignin biosynthesis in phenylpropanoid pathway of transgenic tobacco. *Gene*, *809*, 146017. https://doi.org/10.1016/j.gene.2021.146017

Shin, S., Park, M. S., Lee, H., Lee, S., Lee, H., Kim, T. H., & Kim, H. J. (2021). Global trends in research on wild-simulated ginseng: Quo vadis? *Forests*, *12*(6), 664. https://doi.org/10.3390/f12060664

Solano, R., Stepanova, A., Chao, Q., & Ecker, J. R. (1998). Nuclear events in ethylene signaling: A transcriptional cascade mediated by ETHYLENE-INSENSITIVE3 and ETHYLENE-RESPONSE-FACTOR1. *Genes & Development*, *12*(23), 3703–3714. https://doi.org/10.1101/gad.12.23.3703

Van Breemen, N., Mulder, J., & Driscoll, C. (1983). Acidification and alkalinization of soils. *Plant and Soil*, *75*, 283–308. https://doi.org/10.1007/BF02369968

Vasilev, J., Mix, A. K., Heimerl, T., Maier, U. G., & Moog, D. (2022). Inferred subcellular localization of peroxisomal matrix proteins of Guillardia theta suggests an important role of peroxisomes in cryptophytes. *Frontiers in Plant Science*, *13*, 889662. https://doi.org/10.3389/fpls.2022.889662

Verma, V., Ravindran, P., & Kumar, P. P. (2016). Plant hormone-mediated regulation of stress responses. *BMC Plant Biology*, *16*, 86. https://doi.org/10.1186/s12870-016-0771-y

Vos, I. A., Verhage, A., Schuurink, R. C., Pieterse, C. M., & Van Wees, S. C. (2013). Onset of herbivore-induced resistance in systemic tissue primed for jasmonate-dependent defenses is activated by abscisic acid. *Frontiers in Plant Science*, *4*, 62009. https://doi.org/10.3389/fpls.2013.00539

Wan, Y., Kertesz, M., Spitale, R. C., Segal, E., & Chang, H. Y. (2011). Understanding the transcriptome through RNA structure. *Nature Reviews. Genetics*, *12*(9), 641–655. https://doi.org/10.1038/nrg3049

Wang, Q., Sun, H., Xu, C., Ma, L., Li, M., Shao, C., Guan, Y., Liu, N., & Liu, Z. (2019). Analysis of rhizosphere bacterial and fungal communities associated with rusty root disease of Panax ginseng. *Applied Soil Ecology*, *138*, 245–252. https://doi.org/10.1016/j.apsoil.2019.03.012

Wang, Q., Xu, C., Sun, H., Ma, L., Li, L., Zhang, D., & Zhang, Y. (2016). Analysis of the relationship between rusty root incidences and soil

properties in Panax ginseng. *IOP Conference Series: Earth and Environmental Science, Shanghai, China*, *41*(1), 23–26.

Wei, X., Wang, X., Cao, P., Gao, Z., Chen, A. J., & Han, J. (2020). Microbial community changes in the rhizosphere soil of healthy and rusty Panax ginseng and discovery of pivotal fungal genera associated with rusty roots. *BioMed Research International*, *1*, 1–13. https://doi.org/10.1155/2020/8018525

Xiao, X., Yang, F., Zhang, S., Korpelainen, H., & Li, C. (2009). Physiological and proteomic responses of two contrasting Populus cathayana populations to drought stress. *Physiologia Plantarum*, *136*(2), 150–168. https://doi.org/10.1111/j.1399-3054.2009.01222.x

Xu, F. Q., & Xue, H. W. (2019). The ubiquitin-proteasome system in plant responses to environments. *Plant, Cell & Environment*, *42*(10), 2931–2944. https://doi.org/10.1111/pce.13633

Yana, Q., Min, Y., & Qun, Z. (2017). Functional regulation of plant NADPH oxidase and its role in signaling. *Plant Signaling & Behavior*, *12*(8), e1356970. https://doi.org/10.1080/15592324.2017.1356970

Yang, D. C., Kim, Y. H., Yun, K. Y., Lee, S. S., Kwon, J. N., & Kang, H. M. (1997). Red-colored phenomena of ginseng (Panax ginseng CA Meyer) root and soil environment. *Koryo Insam Hakhoechi*, *21*(2), 91–97.

Zhang, Y., Wang, Q., Xu, C., Sun, H., Wang, J., & Li, L. (2016). Iron (Fe2+)-induced toxicity produces morphological and physiological changes in roots in Panax ginseng grown in hydroponics. *Toxicological and Environmental Chemistry*, *98*(5–6), 630–637. https://doi.org/10.1080/02772248.2015.1133385

Zhao, G., Pei, Y., Yang, R., Xiang, L., Fang, Z., Wang, Y., Yin, D., Wu, J., Gao, D., Yu, D., & Li, X. (2022). A non-destructive testing method for early detection of ginseng root diseases using machine learning technologies based on leaf hyperspectral reflectanc. *Frontiers in Plant Science*, *13*, 1031030. https://doi.org/10.3389/fpls.2022.1031030

Zhao, Q., Cui, M. Y., Levsh, O., Yang, D., Liu, J., Li, J., Hill, L., Yang, L., Hu, Y., & Weng, J. K. (2018). Two CYP82D enzymes function as flavone hydroxylases in the biosynthesis of root-specific 4′-deoxyflavones in Scutellaria baicalensis. *Molecular Plant*, *11*(1), 135–148. https://doi.org/10.1016/j.molp.2017.08.009

Zhao, Y. (1998). New progress in diagnosis and comprehensive management of ginseng rusty root symptoms in Changbai Mountain. *Special Wild Economic Animal and Plant Research*, *1998*(01), 41–46. In Chinese

Zhao, Y., & Li, X. (1998). On the damage of Al3+ in soils to ginseng. *Special Wild Economic Animal and Plant Research*, *03*, 38–42.

Zhao, Y., Liu, J., Guo, J., & Li, X. (1999). The precipitate of epdermis ginseng red coating root were observed with scanning micrograph. *Special Wild Economic Animal and Plant Research*, *1*, 26–27. (In Chinese)

Zheng, L., Lu, G., Pei, W., Yan, W., & Jiang, Q. (2021). Understanding the relationship between the structural properties of lignin and their biological activities. *International Journal of Biological Macromolecules*, *190*, 291–300. https://doi.org/10.1016/j.ijbiomac.2021.08.168

Zhou, Y., Yang, Z., Gao, L., Liu, W., Liu, R., Zhao, J., & You, J. (2017). Changes in element accumulation, phenolic metabolism, and antioxidative enzyme activities in the red-skin roots of Panax ginseng. *Journal of Ginseng Research*, *41*(3), 307–315. https://doi.org/10.1016/j.jgr.2016.06.001

SUPPORTING INFORMATION

Additional supporting information can be found online in the Supporting Information section at the end of this article.

How to cite this article: Yu, P., Song, X., Zhang, W., Yao, Y., Ren, J., Wang, L., Liu, W., Meng, Z., & Meng, X. (2024). Analysis of ginseng rusty root symptoms transcriptome and its pathogenesis directed by reactive oxygen species theory. *Plant Direct*, *8*(5), e586. https://doi.org/10.1002/pld3.586